

Deformation Effects in Hot Rotating ^{46}Ti Probed by the Charged Particle Emission and GDR γ -Decay

M. Brekiesz^a, A. Maj^a, M. Kmiecik^a, K. Mazurek^a, W. Męczyński^a, J. Styczeń^a,
K. Zuber^a, P. Papka^{bc}, C. Beck^b, F. Haas^b, V. Rauch^b, M. Rousseau^b,
A. Sánchez i Zafra^b, J. Dudek^b and N. Schunck^{ad}

^aThe H. Niewodniczański Institute of Nuclear Physics, PAN, 31-342 Kraków, Poland

^bIPHC and ULP (Strasbourg I), B.P. 28 F-67037 Strasbourg Cedex 2, France

^ciThemba LABS, 7129 Somerset West, South Africa

^dDepartamento de Física Teórica, Universidad Autónoma de Madrid, Spain

The $^{46}\text{Ti}^*$ compound nucleus, as populated by the fusion-evaporation reaction $^{27}\text{Al} + ^{19}\text{F}$ at the bombarding energy of $E_{lab} = 144$ MeV, has been investigated by charged particle spectroscopy using the multidetector array ICARE at the VIVITRON tandem facility of the IReS (Strasbourg). The light charged particles and high-energy γ -rays from the GDR decay have been measured in coincidence with selected evaporation residues. The CACARIZO code, a Monte Carlo implementation of the statistical-model code CASCADE, has been used to calculate the spectral shapes of evaporated α -particles which are compared with the experimental coincident spectra. This comparison indicates the signature of large deformations (possibly superdeformed and hyperdeformed shapes) present in the compound nucleus decay. The occurrence of the Jacobi shape transition is also discussed in the framework of a newly developed rotating liquid drop model.

1. INTRODUCTION

In the recent years, there has been a large number of both experimental and theoretical studies aimed at understanding the effects of large deformations in the case of light-mass nuclei [1, 2, 3, 4, 5, 6, 7, 8, 9, 10, 11, 12]. The very elongated prolate or triaxial shapes were deduced from the spectra of the Giant Dipole Resonance (GDR) from the decay of $^{45}\text{Sc}^*$ [1] and $^{46}\text{Ti}^*$ [2, 3]. The results were consistent with predictions made within the macroscopic-microscopic approach of the LSD (Lublin-Strasbourg Drop) model [4, 5], in which the large deformations are ascribed to the Jacobi shape transition. The large deformations were also indicated by the measurement of energy spectra and angular distributions of the light charged particles (LCP) originated from the decay of $^{44}\text{Ti}^*$ [6] as formed in two fusion reactions $^{16}\text{O} + ^{28}\text{Si}$ [7] and $^{32}\text{S} + ^{12}\text{C}$ [8]. In addition, a number of superdeformed bands of discrete γ -ray transitions were discovered in selected $N = Z$ α -like nuclei belonging to this mass region (e.g. [9, 10]). In this paper, we focus on the search for extended shapes and for the Jacobi transition of ^{46}Ti with measurements of the LCP and

GDR spectra in coincidence with evaporation residues (ER) for the reaction $^{27}\text{Al} + ^{19}\text{F}$ at a bombarding energy of $E_{lab}(^{27}\text{Al}) = 144$ MeV. In the following the experimental results are presented and their interpretation are discussed within both the statistical [6, 7, 13] and the LSD [5] models.

2. EXPERIMENTAL RESULTS AND INTERPRETATIONS

The experiment was performed at the VIVITRON tandem facility of the IReS Strasbourg (France), using the multidetector array ICARE [6, 14, 15] associated with a large volume ($4'' \times 4''$) BGO detector. The $^{46}\text{Ti}^*$ compound nucleus (CN) was populated at $E^* = 85$ MeV and with $L_{max} \approx 35 \hbar$ by the inverse kinematics reaction 144 MeV ^{27}Al on ^{19}F . High-energy γ -rays from the GDR decay were measured using the BGO detector. The heavy fragments were detected in six gas-silicon telescopes (IC), located at $\Theta_{lab} = \pm 10^\circ$ in three distinct reaction planes. The in-plane detection of coincident LCP's was done using ten triple telescopes (40 μm Si, 300 μm Si, 2 cm CsI(Tl) thick), eighteen two-element telescopes (40 μm Si, 2 cm CsI(Tl) thick), and four gas-silicon telescopes. Further details on the setup and on the calibration procedures can be found in Ref. [12].

2.1. α -particle spectra

The energy spectra of the α -particles emitted in the laboratory frame at the angles $\Theta_{lab} = 45^\circ, 85^\circ, 125^\circ$ in coincidence with $Z = 18, 19, 20$ measured by the IC located at $\Theta_{lab} = 10^\circ$ are shown in Fig. 1 by the solid points. The lines are the results of the analysis performed using CACARIZO, the Monte Carlo version of the statistical-model code CASCADE [13], which is based on the Hauser-Feshbach formalism [14, 15, 16]. The high-energy part of α -particle spectra depends on the final state level density. The level density is calculated using the Rotating Liquid Drop Model (RLDM) [13] and can be changed using different sets of deformability parameters. Larger deformations lower the yrast line and make it more flat, what increases the level density at higher available excitation energy of the final nucleus, thus reduce α -particle energies. In the code, the yrast line is parameterized with deformability parameters δ_1 and δ_2 : $E_L = \hbar^2 L(L+1)/2\mathfrak{S}_{eff}$ with $\mathfrak{S}_{eff} = \mathfrak{S}_{sphere}(1 + \delta_1 L^2 + \delta_2 L^4)$ [14], where \mathfrak{S}_{eff} is the effective moment of inertia, $\mathfrak{S}_{sphere} = (2/5) A^{5/3} r_0^2$ is the rigid body moment of inertia of the spherical nucleus and r_0 is the radius parameter (set equal to $r_0 = 1.3$ fm in the present calculations). In Fig. 2 (left panel) the yrast lines used in the calculations are displayed as solid lines. The standard RLDM yrast line, which in general can be approximated by the rigid body yrast line with small deformation ($\beta = 0.2$), results in the α -particle spectra presented in Fig. 1 as dashed lines. This parametrization does not reproduce well the experimental spectra.

The solid line in Fig. 1 represents the calculations using the yrast line with the deformability parameters ($\delta_1 = 4.7 \times 10^{-4}$, $\delta_2 = 1.0 \times 10^{-7}$) proposed by [6, 7]. This yrast line, labeled in Fig. 2 (left) "quasi-superdeformed" as it resembles the yrast line for the rigid body with a deformation parameter $\beta = 0.6$, reproduces fairly well the experimental spectra for $Z = 18$ and $Z = 19$. Such large deformations needed to explain the level density of the nuclei after evaporation of few particles are actually consistent with the superdeformed bands found in the nuclei with $A \approx 40$ [9, 10, 11].

However, the spectra associated with $Z = 20$, i.e. related to the emission of a single

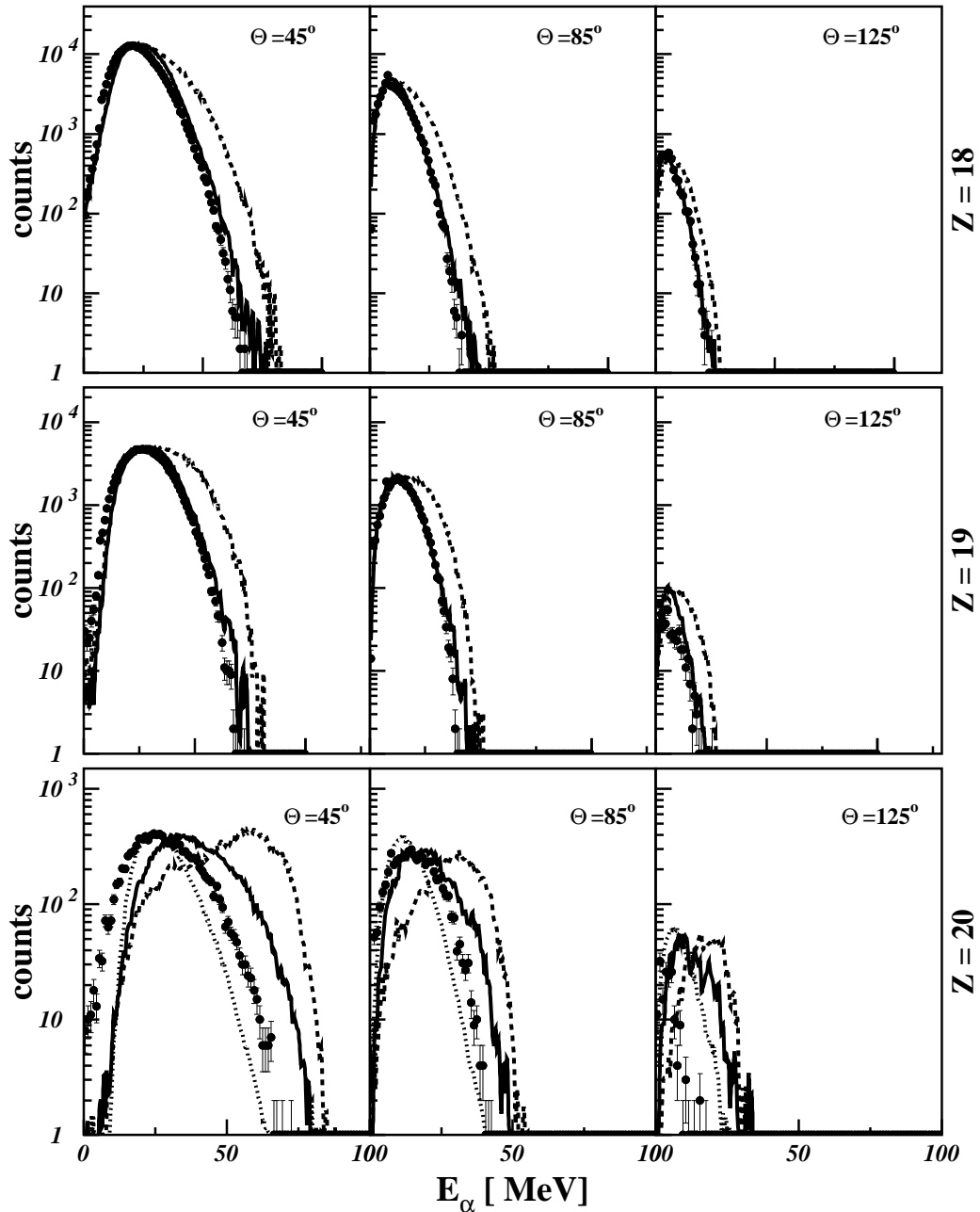


Figure 1. Experimental (points) and calculated (lines) α -particle energy spectra for $\Theta_{lab} = 45^\circ, 85^\circ, 125^\circ$ in coincidence with three different ER's ($Z = 18$: upper row, $Z = 19$: middle row, $Z = 20$: bottom row) detected in the IC at $\Theta_{lab} = 10^\circ$. The calculations were carried out with yrast line deformation parameters from RLDM (dashed line), for quasi-superdeformed shapes (solid line) and for quasi-hyperdeformed shapes (dotted line).

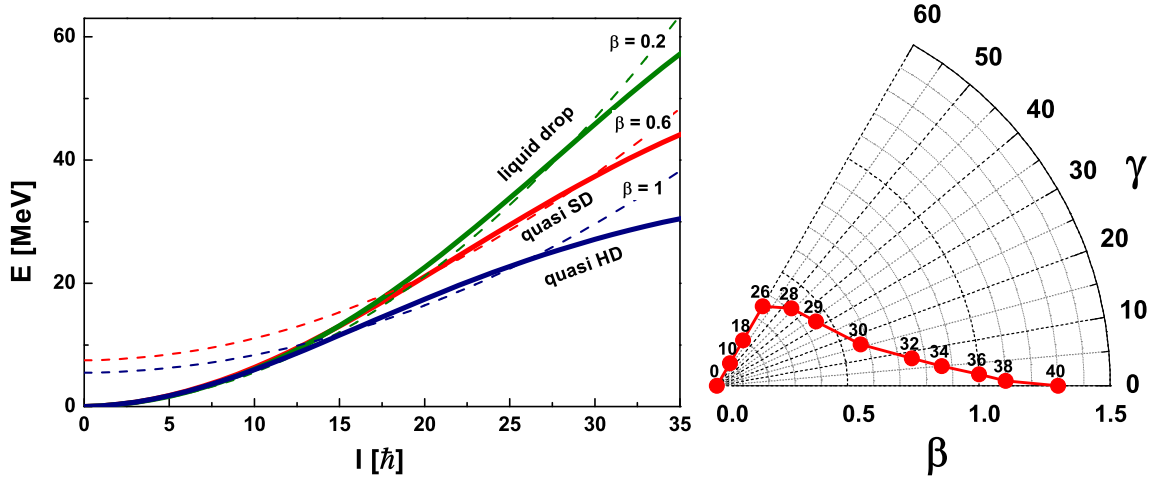


Figure 2. Left: the yrast lines used in the calculations (solid lines) and the rigid body yrast lines with different deformation parameters (dotted lines). Right: the evolution of the equilibrium shape of ^{46}Ti as a function of spin predicted by the LSD model.

α -particle, are still in disagreement with the calculations using the RLDM or "quasi-superdeformed" yrast lines (the slopes of the experimental spectra are larger), despite the fact that in ^{42}Ca highly-deformed band was also found [17], with the properties similar to the superdeformed bands in lower mass α -like nuclei. In order to improve the agreement, an even more deformed yrast line (which mimics an unusual extended shape) would be required. An example of the calculations in which the agreement of the slopes of the spectra is better, even the calculated slopes are too large, is shown for $Z = 20$ with dotted line. These calculations were using the yrast line with the deformability parameters ($\delta_1 = 1.1 \times 10^{-3}$, $\delta_2 = 1.0 \times 10^{-7}$), depicted in Fig. 2 as "quasi-hyperdeformed" as it resembles the yrast line for the rigid body with a deformation parameter $\beta \approx 1$. This result seems to be rather unexpected. Even though according to macroscopic-microscopic calculations made with the LSD model, the equilibrium deformation of the (hot) nucleus ^{46}Ti can be characterized by such extreme deformations at the highest possible spins of the reaction ($I \approx 34-36$), the cooling process performed through particle emission is expected to lead to much smaller deformations. Indeed, at low temperatures shell effects play a prominent role and tend to stabilize the nucleus in near-spherical or at best superdeformed shapes [18]. This is indeed the case when more than one charged particle is emitted (see the spectra for $Z = 18, 19$ in Fig. 1).

A possible explanation can be related to the time scale of the evaporation process. When many particles are evaporated, the time needed for this process can be long enough, so that the residual nucleus changes its shape to smaller deformation and the effective level density of final states can be described by the "quasi-superdeformed" yrast line. In contrast, if only one α -particle is being emitted (the case for $Z = 20$), it is possible that the residual nucleus is still in the process of changing shape. Therefore the appropriate yrast line will have a shape between the shape of CN (with $\beta \approx 1$), i.e. described by

the "quasi-hyperdeformed" yrast line, and a shape of final nucleus, described by the "quasi-superdeformed" yrast line. Such an effect can be understood as an existence of a "dynamical hyperdeformation". Although one cannot exclude another explanation of this anomalous shape of α -particle spectra in coincidence with the residues of $Z = 20$, e.g. spin dependent binding energies, it is worth to mention that analogous explanation was given for the observed α -particle spectra in the decay of ^{59}Cu CN [19].

2.2. GDR strength function from high-energy γ -ray spectrum

The deformation parameters β and γ of the minima in the potential energy surfaces, calculated with the LSD model, are presented in the Fig. 2 (right panel), showing the evolution of the equilibrium shape of ^{46}Ti as function of spin. As angular momentum increases, the nucleus originally spherical at $I = 0$ acquires some oblate deformation, corresponding to an elongation of up to $\beta \approx 0.3$ for $I = 26$. Beyond $26 \hbar$, the Jacobi shape transition sets in: the nucleus becomes triaxial with the elongation parameter increasing up to values of $\beta \geq 1$ for $I = 38$, and the fission finally takes place at $I \approx 40$.

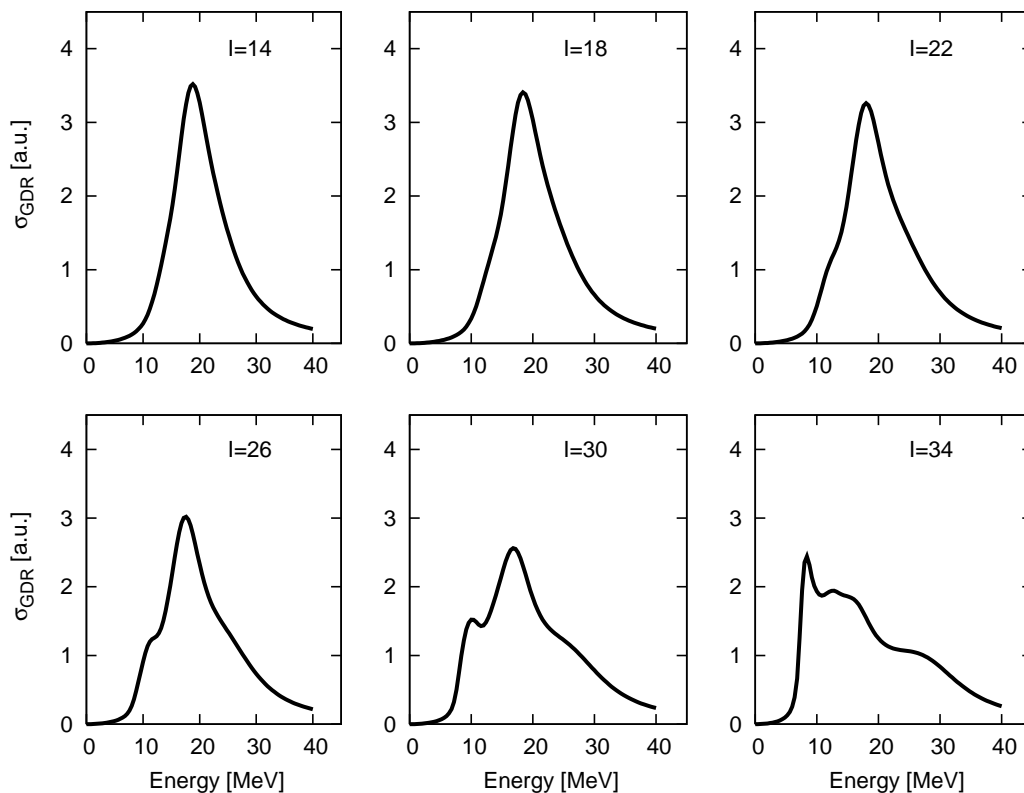


Figure 3. GDR strength functions for ^{46}Ti at different spins simulated by the thermal shape fluctuation model based on the potential energies from the LSD model.

The LSD potential energy surfaces constituted also a basis for the thermal shape fluctuation method to compute the GDR strength functions [5], presented in Fig. 3. For

the oblate regime below $I = 26$ the calculated GDR line shape has the form of a broad Lorentzian distribution. For the Jacobi regime ($I \geq 26$) the line shape is characteristically split forming a narrow low-energy component around 10 MeV, and a broad structure ranging from 15 to 27 MeV. This splitting is a consequence of both the elongated shape of the nucleus undergoing the Jacobi shape transition and strong Coriolis effects [20] which additionally split the low energy component and shift a part of its strength down to 10 MeV. Such fragmented GDR strength function was indeed experimentally observed for ^{46}Ti at highest spins in the EUROBALL+HECTOR experiment [3].

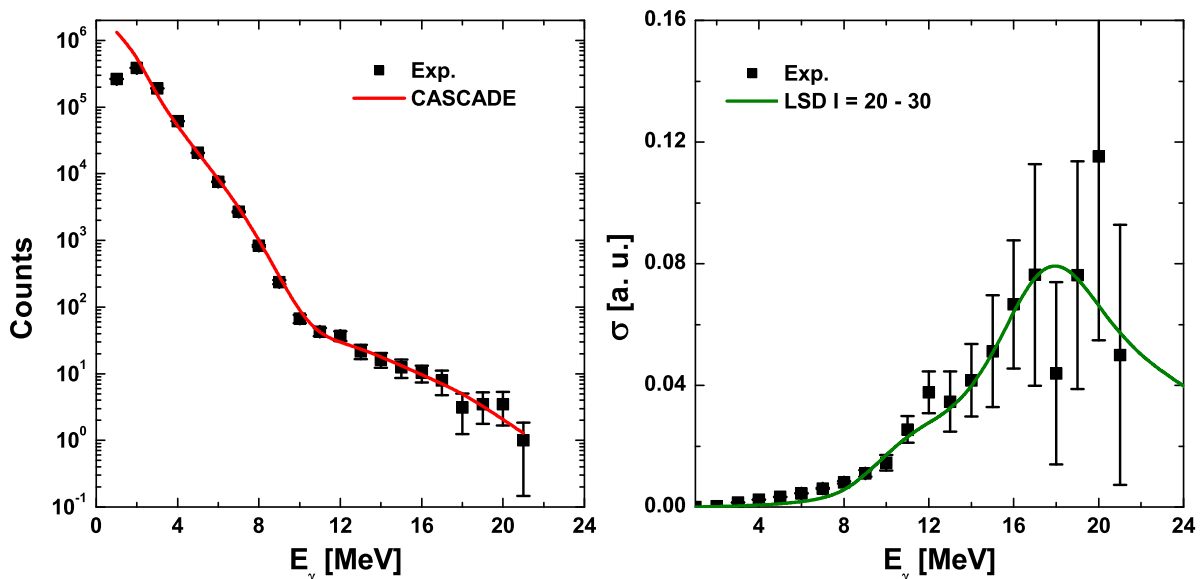


Figure 4. Left: High-energy γ -ray spectrum measured in coincidence with the recoils possessing $Z = 18, 19$ and 20 , together with the best fit CASCADE calculations in which the "quasi-superdeformed" yrast line was used and the GDR parameters that fit the spectrum were $E_{GDR} = 18.5$ MeV, $\Gamma_{GDR} = 14$ MeV and $\sigma_{GDR} = 1$. Right: The extracted GDR strength function (points) together with the LSD model prediction (line) for $I \geq 20$.

In the present experiment there was only very limited way to select the GDR decay related to the highest spins, namely by selecting the coincidences with residues possessing highest $Z = 20$. This was sufficient for the α -particle channel selection although the statistics of the GDR γ -decay was very low. Therefore in order to perform the statistical model analysis the sum of coincidences with Z ranging from 18 to 20 was used. The resulting high energy γ -ray spectrum is shown in Fig. 4 (left panel), together with the CASCADE calculations in which the GDR parameters were fitted. The extracted GDR strength function is shown in the right panel of Fig. 4. Indeed the data do not show any distinct low energy component, but this is consistent with the LSD model prediction, when one takes into account the fact that this spectrum consists of contributions from a broad spin window ($\geq 20 \hbar$).

3. SUMMARY AND OUTLOOK

The spectra of α -particles emitted from hot rotating ^{46}Ti evidence the large deformations ($\beta \approx 0.6$) that are involved in the evaporation process. The process of emission of a single α -particle suggests even larger deformations linked to the effect of "dynamical hyperdeformation". The GDR spectra are also consistent with such large deformations. Unfortunately, the lack of the effective high-spin selectivity in the experiment does not allow us to observe the predicted GDR splitting. However, the global properties of the GDR spectrum of Fig. 4 are fairly well reproduced by the LSD model.

This type of experiments will be attractive with the availability of the intense radioactive beams, since in the more neutron rich nuclei, produced in fusion-evaporation reactions, higher spins can be reached, enabling stronger population of the "Jacobi shapes" window.

This work has been supported by the Polish Ministry of Science and Higher Education (Grant No. 1 P03B 030 30). We thank the VIVITRON staff, J. Devin and M.A. Saettel for the excellent support in carrying out the experiment.

REFERENCES

1. M. Kicińska-Habior et al., *Phys. Lett.* **B308** (1993) 225.
2. A. Maj et al., *Nucl. Phys.* **A687** (2001) 192c.
3. A. Maj et al., *Nucl. Phys.* **A731** (2004) 319.
4. K. Pomorski and J. Dudek, *Phys. Rev.* **C67** (2003) 044316.
5. N. Dubray, J. Dudek and A. Maj, *Acta Phys. Pol.* **B36** (2005) 1161.
6. P. Papka, Ph.D. Thesis, Internal Report IReS **04-07** (2004).
7. P. Papka et al., *Ric. Sc. Educ. Perm. Supp.* **122** (2003) 373; nucl-ex/ **0307002**.
8. P. Papka et al., *Acta Phys. Pol.* **B34** (2003) 2343.
9. E. Ideguchi et al., *Phys. Rev. Lett.* **87** (2001) 222501.
10. C. Beck, *Nucl. Phys.* **A738** (2004) 24; C. Beck, *Int. J. Mod. Phys.* **E13** (2004) 9.
11. C.E. Svensson et al., *Phys. Rev. Lett.* **85** (2000) 2693.
12. M. Brekiesz et al., *Acta Phys. Pol.* **B36** (2005) 1175.
13. F. Pühlhofer, *Nucl. Phys.* **A280** (1977) 267.
14. C. Bhattacharya et al., *Phys. Rev.* **C65** (2002) 014611.
15. M. Rousseau et al., *Phys. Rev.* **C66** (2002) 034612.
16. D. Mahboub et al., *Phys. Rev.* **C69** (2004) 034616.
17. M. Lach et al., *Eur. Phys. J.* **A16** (2003) 309.
18. A. Maj et al., *AIP Conference Proceedings* **85** (2005) 264.
19. B. Fornal et al., *Phys. Rev.* **C40** (1989) 664.
20. K. Neergård, *Phys. Lett.* **B110** (1982) 7.